Title

THE EFFECT OF PLASTIC STRAINING AND CYCLIC HEATING ON THE MARTENSITIC TRANSFORMATION IN AN ALLOY STEEL

Author

Dickson, David T.

Publication Date

1964-06-01

UCRL-11388

University of California

Ernest O. Lawrence Radiation Laboratory

THE EFFECT OF PLASTIC STRAINING AND CYCLIC HEATING ON THE MARTENSITIC TRANSFORMATION IN AN ALLOY STEEL

DISCLAIMER

UCRL-11388

UNIVERSITY OF CALIFORNIA

Lawrence Radiation Laboratory
Berkeley, California

AEC Contract No. W-7405-eng-48

THE EFFECT OF PLASTIC STRAINING AND CYCLIC HEATING ON THE MARTENSITIC TRANSFORMATION IN AN ALLOY STEEL

David T. Dickson

(M.S. Thesis)

June 1964

UCRL-11388

THE EFFECT OF PLASTIC STRAINING AND CYCLIC HEATING ON THE MARTENSITIC TRANSFORMATION IN AN ALLOY STEEL

David T. Dickson

Inorganic Materials Research Division, Lawrence Radiation Laboratory
and Department of Mineral Technology, University of California
Berkeley, California

ABSTRACT

A thermal-mechanical process was developed to produce a fine alloy carbide dispersion in a high carbon steel (0.86C, 9.78Cr). A dislocation grid was first produced by warm-working the austenite to produce a dislocation network. Alloy carbides were precipitated on the network during the warm-working operation. The initial martensite plates were limited in size since they were confined to the carbide-dislocation grid. The remaining austenite in this alloy was then completely converted to martensite by a series of alternate elevated and progressively decreasing cryogenic temperature treatments. The result was a fine dispersion of alloy carbides in a matrix of fine grained hard (Rc 65) martensite.

I. THEORY

According to Orowan[1] the shear strength (τ) of a dispersion hardened material is equal to:

$$\tau = \frac{\mu b}{\lambda - d} \qquad (1)$$

where μ = shear modulus of the matrix

b = Burgers vector of the matrix

λ = center to center spacing of the dispersed particles

and d = particle diameter.

The above equation assumes that the particles are spherical and are spaced in a uniform three-dimensional dispersion, and that the particles will not fracture under an applied stress. A three-dimensional network prohibits dislocation climb, and therefore yielding will take place by dislocations bowing between the dispersed particles. Since the shear modulus and the Burgers vector in Eq. (1) cannot be altered to any great extent, the only method of increasing the yield strength is to decrease the particle spacing λ. Turkalo and Low[2] have found a linear relationship between the log of the interparticle spacing and the yield strength. Although this is not in agreement with Eq. (1), the fine alloy carbide spacing in the steel studied by Turkalo and Low were found to increase the yield strength. This report deals with the use of known mechanical processing techniques on an alloy steel in order to produce a three-dimensional alloy carbide dispersion.

McEvily and Bush[3] proposed that alloy carbides were nucleated during the deformation of austenite in the ausform* process. Recent work by McEvily, Bush, Schaller, and Schmatz[4] has shown that the major contribution to the increase in strength of the ausformed steels is due to alloy carbides which were formed during deformation of the austenite. These carbides were inherited by the subsequently formed martensite.[4] The size and distribution of these carbides depend on the dislocation structure of the deformed austenite. The alloy carbide particles were not coherent with the martensite due to the change in volume of the martensite formed in the austenite to martensite transformation.

Deformation of austenite at warm working temperatures tends to make the dislocations line up into bands. During the deformation, there is an increased diffusion rate of carbon and chromium. This increased rate is due to the presence of vacancies formed during the deformation. At the temperature of deformation, the carbon and chromium atoms will tend to move to more favorable energy sites. The more favorable energy site is in the highly disoriented dislocation bands. The result is a network of alloy carbides in these bands. The alloy carbide network will reduce the size of the martensite plates. This is because the martensite plates are not able to penetrate the carbide-dislocation network.[4-6] This method of limiting the martensite plates was proposed by Schmatz, Schaller, and Zackay.[5]

---

* Ausforming is the deformation of metastable austenite prior to transformation to martensite and/or bainite.

A random dislocation network can be used to produce nucleation sites for alloy carbides. It has been found by Wilson[7] that the deformation of martensite will produce nucleation sites for alloy carbide precipitation. The carbon and chromium atoms migrate to the dislocations. When enough carbon and chromium atoms have associated (in a carbon atmosphere or Cottrell atmosphere), a stable carbide nucleus will be formed.[8]

In the present study, the above concepts were used to produce a microstructure with a finely dispersed alloy carbide network. A combination of various known heat treatments was used to produce an alloy carbide dispersed phase microstructure. First, the austenite was defomed at temperatures near 500°C. The purpose of this warm working operation was to produce a grid structure of fine dislocation bands. This temperature was chosen because the dislocations are mobile and tend to segregate in an array, rather than a random dispersion. Also, the spacing of the dislocation arrays is such that the austenite is divided into small cells. This temperature was also chosen because it has been shown that fine carbides precipitate on the dislocation network at temperatures near the normal tempering temperature. After dislocation arrays are formed, carbon and chromium atoms will diffuse to the arrays and will segregate due to favorable strain energy considerations. When a carbon atmosphere has been formed in the vicinity of the dislocation network, stable alloy carbides will be nucleated.

After the warm working, the austenite is quenched to a temperature slightly below the Ms in order to form a volume of martensite. The martensite plates so formed are small because they are trapped in the alloy

carbide-dislocation grid. Some of the alloy carbides which are formed inside the carbide-dislocation grid are now trapped in the martensite plates. When the martensite plates form, dislocations are formed in the austenite due to the change in volume of the martensite plates relative to the untransformed austenite.

The specimen is then tempered to allow alloy carbides to nucleate and grow on the dislocations. These alloy carbide particles will nucleate and grow both inside the martensite plates and in the matrix. The specimen is then quenched to a temperature below the previous quench, forming another burst of martensite plates. These plates also inherit the alloy carbides from the austenite, and the process is continued over again. Figure 1 shows a pictorial summary of the heat treatment.

The final result of the above processing should be small martensite plates trapped inside a alloy carbide-dislocation grid. These plates should contain precipitated alloy carbides which were either (1) nucleated in the austenite by the deformation due to the rolling or from the transformation of the austenite to martensite, or (2) precipitated on dislocations in the martensite.

The fine three-dimensional alloy carbide precipitate in the tempered martensite matrix should have a high yield strength due to the blocking of dislocations. By careful processing, the size and distribution of the precipitate can be controlled to an extent which will have a large effect on the interparticle spacing value in Eq. (1).

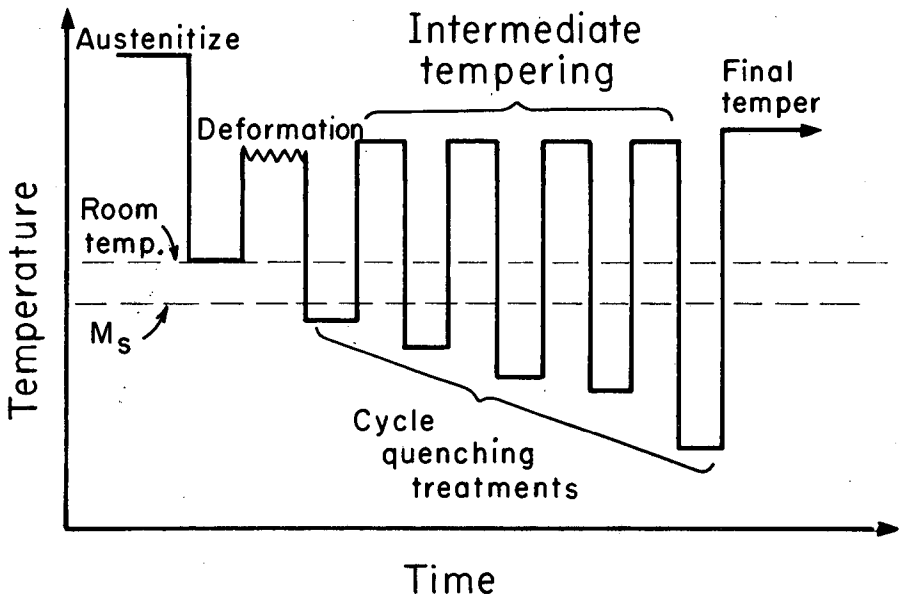

Fig. 1. Schematic representation of proposed thermal-mechanical treatment.

II. EXPERIMENTAL PROCEDURE

A. Specimen Composition and Size

The composition of the specimen used in the experiment is as follows:

C	Cr	Mn	S	Si	Ni
0.86	9.78	0.74	0.010	0.59	0.033

O_2	N_2	H_2
0.0055	0.0101	0.00013

Ingots were made by melting by induction heating in a pressure of 0.9 atm. helium. Ingots of approximately $2\frac{1}{2}$" in diameter and 10" in length were poured. The weight of the ingot was approximately 2,000 grams. The ingot was then forged to 3/8" by 9/16". After forging, the ingots were ground to 0.310" by 0.500" bar stock, and a sample taken for chemical analysis. The bar stock was then cut into 6" lengths for easier handling, and sealed in quartz tubes under a pressure of 1/7 atm of argon. The bar stock was then austenitized at 1200°C (2192°F) for two hours in order to insure homogeneity and large grain size. The bar stock was air cooled from the austenitizing temperature while still in the quartz tubes. The specimens were then examined metallographically and by x-ray analysis. This was done in order to insure that the samples were essentially 100% austenite, and that there was no liquification at the austenitizing temperature.

B. Rolling Technique

The bar stock was cut into various lengths depending on the amount of deformation proposed. The lengths were cut so that the final specimen length after rolling would be approximately 6-in. The specimens to be rolled were sealed in $\frac{1}{2}$-in. diam, 109 mil wall stainless steel tubing. The tubing served two purposes. First, to keep the specimen surface from oxidizing during the high temperature rolling. Second, the tubing was an effective heat sink for the specimen at high temperatures.

The specimens were heated in a tube furnace prior to and between passes of the rolling operation. A preheat time of 15 minutes was used prior to the rolling operating in order to bring the stainless steel clading and the specimen up to the rolling temperature. Deformation was taken in steps of 25 mils per pass during the initial stages of deformation, and 15 mils per pass at the final stages of deformation. After two passes through the rolling mills, the specimen was returned to the furnace for a period of approximately three minutes. The total time of deformation for the 85% reduction in area was less than one hour. After the last pass through the rolling mills, the specimen was quenched in water in order to retain the austenite phase at room temperature.

The specimens were then freed from the stainless steel jacket and ground to the desired shape for metallographic, x-ray, or tensile tests. The specimen was flooded with coolant during the grinding operation. This was done in order to insure the absence of grinding checks, and also to prevent transformation due to excessive heating during grinding.

C. Quench and Tempering Operation

Since the M_s of this alloy was well below room temperature, the heat treatment of the as deformed alloy was not difficult. Ethanol was used as a quenching medium. Liquid nitrogen was added to the alcohol in order to achieve lower temperatures. Since the M_f of this alloy was found to be well above the freezing point of the alcohol, only this quenching medium was used. However, a liquid nitrogen quench was used to try to eliminate the retained austenite. The quenching bath was stirred mechanically, and the temperature was measured using a potentiometer and an iron vs. constantan thermocouple. Since a large amount of liquid was used in the quenching bath, it was possible to achieve close temperature control. Stirring the bath was necessary in order to minimize the temperature gradient.

The tempering bath consisted of nitrates in a resistance heated salt pot. The specimen was quenched from the salt bath into water after each tempering treatment. The temperature variation of the salt bath was approximately ± 2°C.

D. Measurement of Phase Transformation

The original method used for measurement of the extent of transformation was a Rockwell hardness tester. The C scale was used (150 Kg. with Braile indenter) due to the high hardness of the as deformed austenite and the martensite. The hardness ranged from Rc 32 for the austenite at small amounts of deformation to Rc 65 for the martensite formed from heavily deformed austenite. The Rockwell C scale is also

useful because there is a correlation between the hardeness values and tensile strength (although this breaks down in marteniste formed from deformed austenite). This process allowed the use of easily obtainable hardness data rather than making tensile specimens for each variation in heat treatment.

A more accurate method of determining the extent of transformation was needed. A measurement of the permeability of the partially transformed alloy vs. the equilibrium structure (ferrite and alloy carbides) was tried. Two sets of identical coils were used. An identical voltage was passed through the primary coils, and the secondary coils were connected in opposition to each other. The secondary coils were balanced so that a null point was reached (i.e., equal voltages). With the coils in the null position, a specimen of the equilibrium structure was placed inside one of the coils as a standard. The increase in the voltage due to the standard was used as a reference for "100% transformation". The standard specimen was removed, and the unknown specimen put in its place. The ratio of the resulting output voltage to the output voltage for the standard was taken to be the ratio of the transformed to the untransformed material. The size of all of the specimens was standardized in order to eliminate the differences in voltage due to differences in volume of the samples. [The wiring diagram is included in Appendix A].

This method has some drawbacks. Its simplicity lies in the fact that the austenite is paramagnetic, whereas the martensite is ferromagnetic and has a high permeability. The drawback of this technique is that the magnetic field used does not saturate the specimen. This means that the ratio between the martensite and the equilibrium structure (of ferrite

and alloy carbides) cannot be determined. Therefore, an arbitrary ratio of 1 to 1 was used.

A third, and more time consuming method of determining the extent of transformation is x-ray analysis. Its drawbacks are obvious. First, the setup time is much longer than for the two previous methods. The conditions under which it is used must remain constant. Second, the amount of tetragonal martensite cannot be found by direct comparison of the total x-ray intensity. Only the integrated intensities can be compared. This is a long and tedious process, and does not compare to the simplicity of the two previous methods. This method was used only in the final heat treatment.

E. Strength Measurements

As was mentioned previously, the relative strength of each treatment could be determined by hardness measurements. After the effects of most of the variables had been determined, samples were made for bend tests. Four point loading was used rather than the more conventional three point. Four point bending was chosen because of its superiority in determining small amounts of ductility.

For a final evaluation of the processing, tensile specimens were used. Specimens 4-in. long with a 1-7/8 in gauge length were used. [The specimen dimensions can be found in Appendix B.] Because of the high hardness of the specimen, low carbon steel sheets were fastened to the specimen with Eastman E-410 epoxy resin. The low carbon steel was fastened so that it would be between the grips of the tensile machine and the specimen. Tensile tests were run in an Instron testing machine

with a crosshead travel speed of 0.010 cm/minute.

III. EXPERIMENTAL RESULTS

A. Deformation Temperature and Amount

The first objective of this study was to refine the martensite plate size through various thermal-mechanical treatments. The method used was to obtain a fine dislocation grid by using various combinations of rolling temperature and amounts of deformation. Next, a fine carbide precipitate was formed on the dislocation network which was formed during rolling. The dislocation network would limit the size of the martensite plates by acting in a way similar to austenite grain boundaries. In effect, the "austenite grain size" would be reduced to the cell size of the area between the carbide-dislocation substructure.

Five deformation temperatures were chosen (370, 400, 430, 460, and 490 °C), along with three amounts of reduction in area (50, 70, and 85 %). Optical metallography was used after deformation to determine the mode of carbide-dislocation substructure due to each of the above mentioned parameters. The specimens were then quenched in order to determine the effectiveness of the substructure in limiting the martensite plate size. Optical metallography showed that as the deformation temperature increased, the distance between the dislocation bands increased, and the carbide precipitation in these bands also increased. Figure 2 shows that the initial martensite plate length decreased as the deformation temperature increased. This shows that although the width between the dislocation bands increased with increasing temperature, the effectiveness of the bands

to limit martensite plate size increased with temperature. This was probably due to the larger amounts of precipitated alloy carbides at higher deformation temperatures. Figure 2 also shows a general trend toward decreased plate size with larger amounts of deformation. This is because the number of dislocation bands, increased, and the spacing between bands decreased with increasing amounts of deformation.

Figure 3 shows the effect of deformation on the hardness of as-rolled austenite. The hardness increased as the austenite work hardens, but then trends to fall off at higher amounts of deformation. This is due to the presence of austenite decomposition products at higher deformation temperatures. These austenite decomposition products can be seen metallographically (see Fig. 13), and they can also be determined by the use of a magnet. The austenite decomposition is accelerated due to the high concentration of vacancies in the deformed austenite which enhance diffusion. Austenite decomposition is enhanced by the longer times at the deformation temperature needed for larger amounts of deformation.

The second step in choosing the amount and the temperature of deformation was finding if there was any tendency toward austenite stabilization due to any particular processing technique. A standard cycling treatment was used, consisting of ten intermediate quenches between the M_s (of the undeformed alloy) and -196°C. Each of these quenches was followed by a tempering treatment at 490°C (914°F) for ten minutes. Figure 4 shows the effect of rolling temperature on the percent austenite decomposition* to martensite by cycle quenching. By correlating the

---

* Determined in the magnetic apparatus.

microstructures with the data, it would seem that the fine dislocation network seems to prevent the martensite from forming (i.e., stabilizes the deformed austenite). The higher amounts of deformation seem to enhance transformation. This is probably due to the formation of nucleation and growth transformation products, thereby lowering the carbon content of the remaining austenite. Also, there are more regions of low dislocation density, due to the higher density of the dislocations in the dislocation network. Another explanation is that the M_s increases with increasing amounts of deformation due to the strain induced formation of the martensite. All of the above can be used to explain the curves in Fig. 5. It can be seen that the start of transformation from austenite to martensite increases with increasing amounts of deformation and with increasing temperature. It should also be noted that the M_s of the deformed alloy is higher than the M_s of the undeformed alloy. The effect of two different amounts of deformation on stabilization (and hence the M_s) is shown in Fig. 6. These data seem to show that while the 70% deformation has achieved its maximum hardness at -75°C (-103°F), and is in fact starting to temper, the 50% reduction in area was not able to achieve its maximum potential due to some stabilization phenomenon. As a comparison, the transformation curve and the M_s for the undeformed specimen are also shown.

B. Cycling Temperature and Time

The purpose of the cycle tempering treatment is to induce carbide precipitation on the dislocations in the untransformed austenite and newly transformed martensite. These dislocations result from the plastic

deformation of the austenite due to the change in volume of the martensite relative to the parent austenite. Since the carbide formation is a nucleation and growth process, it is dependent on the diffusion rate of the carbon and the chromium. Because the carbon and chromium diffusion rate is proportional to temperature and time to the one-half power, the less important variable, time was held constant at ten minutes, while the temperature was varied to produce the desired alloy carbide precipitation.

Figure 7 shows the effect of increasing the cycle tempering temperature on the final hardness of the alloy. There is a slight change in the final hardness from a change in cycle tempering temperature of 490°C (914°F) to 535°C (995°F). There is a sharp drop in hardness when the specimen is overtempered. The microstructure showed that the carbides in the 580°C (1076°F) range and above are continuous, although not massive. At this point in the experiment, strength and ductility tests were made in order to determine the effect of various parameters on the ductility. Because of the need of determining small amounts of ductility, tests of four point load bend tests were used rather than tensile tests. The result of these tests can be found in Table I. The material, 85% deformed at 490°C (914°F), proved to be the most ductile and was therefore used in all subsequent work.

C. Final Tempering Temperature

A final series of tests was made in order to determine the best final tempering temperature. The optimum tempering temperature would be that temperature which would give a reasonable amount of ductility

while retaining high strength.

As in the previous tests, a reduction of 85% at 490°C (914°F) was used for the deformation treatment. Then two identical cycling treatments were made except that two different cycling temperatures were used. Because the ausform materials show a high degree of resistance to tempering at the deformation temperature, two temperatures slightly above the rolling temperature were chosen. The results of these tests are shown in Fig. 8. Metallography of the two microstructures showed that the carbides in the 520°C (968°F) tempered specimen were somewhat more coarse than the 500°C (932°F) specimen. No undesirable carbide agglomeration was found in either specimen.

After the cycling treatment, a final tempering treatment was used. Three different temperatures were chosen. One temperature was the usual tempering temperature for this alloy, and the other two temperatures were slightly below and slightly above this temperature. However, all of the final tempering temperatures chosen were above the highest cycle tempering temperature. Figures 9 and 10 show the effect of tempering time at these three temperatures on the hardenss of the two specimens. The higher cycling temperature specimens showed a greater softening rate than the specimens cycled at 500°C (932°F). The reason for this was obvious when the microstructures of these specimens were examined. The carbides in the 520°C (960°F) cycled specimen were more gross at each hardness level than those of the 500°C (932°F) specimen. For this reason, the 520°C (968°F) cycled specimen was rejected, even though it had an initial hardness greater than the 500°C (932°F) cycled specimen.

The microstructures of the 500°C (932°F) cycled specimen were then examined during the final tempering treatment at various hardness levels. It was found that the growth of carbides was minimized by the use of longer times at the lowest final tempering temperature of 530°C (986°F), rather than short times at the higher final tempering temperatures of 545°C (1013°F) and 560°C (1040°F).

D. Final Treatment

A final treatment was devised using the results of the previous experiments. This treatment gave the best microstructure in that the carbides were distributed in a fine dispersion. Figure 11 shows the rolling and cycle temper treatment used. The marked points in Fig. 11 are correlated with the optical micrographs in order to show the progression of the microstructure at various stages in the treatment.

Figure 12 shows the as-rolled austenite. Some evidence of isothermal transformation can be seen in the microstructure. This is correlated with the slight magnetic susceptibility of the as-rolled austenite, proving the formation of magnetic constituents. The elongated austenite grains can be seen with some decomposition in the grain boundaries. The carbides in the slip bands are not visible, but they can be seen in later photomicrographs. The hardness of this specimen is R_c 58.4.

Figure 13 shows the specimen after the -20°C (-4°F) quench and temper treatment. Some martensite is formed in isolated areas of the microstructure. The hardness of the specimen is R_c 58.7.

Figure 14 shows the specimen after the -40°C (-40°F) quench and temper. More martensite is evident, and the martensite formed from the initial quench is shown darker than the fresh martensite, due to the longer tempering time. The martensite plates seem to be trapped in some manner, but the evidence of the decorated slip bands is not evident here. The hardness of this specimen is R_c 60.5.

Figure 15 shows the specimen after the -60°C (-76°F) quench and temper. The fresh martensite appears lighter than the martensite initially transformed. The hardness of this specimen is R_c 61.5.

Figure 16 shows the specimen after the -80°C (-112°F) quench and temper. The transformation is nearly completed. The decorated slip lines are seen to stop the propagation of the martensite plates. The hardness of this specimen is R_c 62.7.

Figure 17 shows the specimen after the -196°C (-321°F) quench. According to x-ray measurements, this alloy is approximately 100% martensite. The hardness of this specimen is R_c 63.9.

Figure 18 shows the undeformed austenite which was cycled in the same manner as the rolled austenite. Note the initial martensite plates which appear darker due to the longer tempering time. Also note the random orientation of the plates. The hardness of this specimen is R_c 54.7.

Figure 19 shows the as rolled austenite given a direct quench to -196°C (-321°F) with no cycling or tempering treatment. Note the large austenite grain size (almost the entire area of the micrograph), and the small martensite plates running between the decorated slip bands. The hardness of this specimen is R_c 63.9.

Figure 20 shows the undeformed specimen direct quenched to -196°C. The hardness of this specimen is R_c 58.2.

Figure 21 shows the deformed specimen after cycle quenching to -196°C (986°F) for one hour. The appearance of this microstructure is similar to that of the cycle quenched to -196°C (-321°F), (Figure 17), except that the martensite appears darker due to the final tempering treatment. There is no undesirable carbide agglomeration present at this stage of the final tempering treatment. The hardness of this specimen is R_c 61.6.

Figure 22 shows the same specimen as Fig. 21 except for a final tempering treatment of three hours. Note the fine carbide dispersion except for the presence of some undesirable carbide agglomeration. The hardness of this specimen is R_c 59.7.

Figure 23 shows the same specimen as Fig. 21 except for a final tempering treatment of five hours. Note the presence of undesirable carbide agglomeration. This alloy is definitely in the over tempered condition. The hardness of this specimen is R_c 57.6.

Figure 24 shows the same specimen as Fig. 21 except for a final tempering treatment of seven hours. The microstructure is dominated by a dense carbide network. The hardness of this specimen is R_c 54.1.

Figure 25 shows a specimen which was rolled 70% at 460°C (860°F), and cycled at 490°C (914°F) to -196°C (-321°F). Although this specimen shows the best microstructure because of the small martensite plate size, bend tests showed this specimen to be brittle in the untempered condition. The hardness of this specimen is R_c 61.6. This is the maximum hardness achieved with this specimen. Its low hardness value could be due to the presence of retained austenite.

Figure 26 shows the hardness of this final tempering treatment with time. The tempering treatment is correlated by the microstructures. Tempering this alloy to improve ductility proves useless due to the growth of massive carbide networks.

All of the tensile specimens broke in a brittle manner before the elastic limit of the material could be reached.

IV. CONCLUSIONS

There are a number of conclusions that can be drawn from this experiment.

(1) The initial martensite plate length decreases as the deformation temperature increases, due to the interaction with the dislocation bands. Although the spacing of the dislocation bands increased with temperature, the effectiveness of the bands to limit the martensite plate size increased with temperature. This was due to heavier alloy carbide precipitation on the dislocation bands at the higher deformation temperatures.

(2) The austenite hardness increased as the amount of deformation increased. This hardness increase is believed due to the increased rate of nucleation of isothermal decomposition products. The increase in nucleation rate was probably due to the greater number of nucleation sites and possibly due to the enhanced diffusion occasioned by higher vacancy concentration.

(3) The cycling temperature which was just above the deformation temperature produced the best alloy carbide dispersion, although it did not give the highest hardness.

(4) The final tempering temperature, which was just above the deformation temperature, gave the best alloy carbide dispersion, although some carbide agglomeration could not be prevented.

(5) The optimum microstructure was produced by the controlled nucleation and growth of alloy carbides, and the complete conversion of the austenite to a fine grained martensite. The maximum hardness of the microstructure was R_c 65.

V. RECOMMENDATIONS

(1) A new series of alloys should be made with a lower carbon content. This would reduce the amount of alloy carbide agglomeration in the tempered structure.

(2) The size of the alloy carbides that precipitate must be kept at a minimum. This might be accomplished by reducing the diffusivity of the carbide-forming elements. Alloying elements such as Mo, W, V, Ti, etc. should be substituted in part for the chromium used in the present investigation.

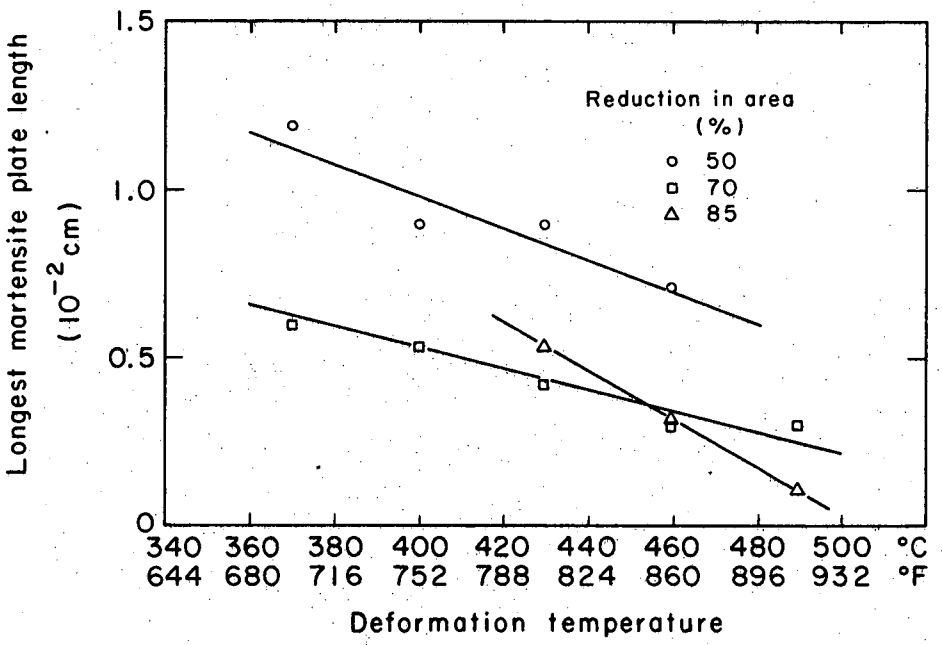

Fig. 2. The effect of deformation temperature and percent reduction in area on the initial martensite plate length.

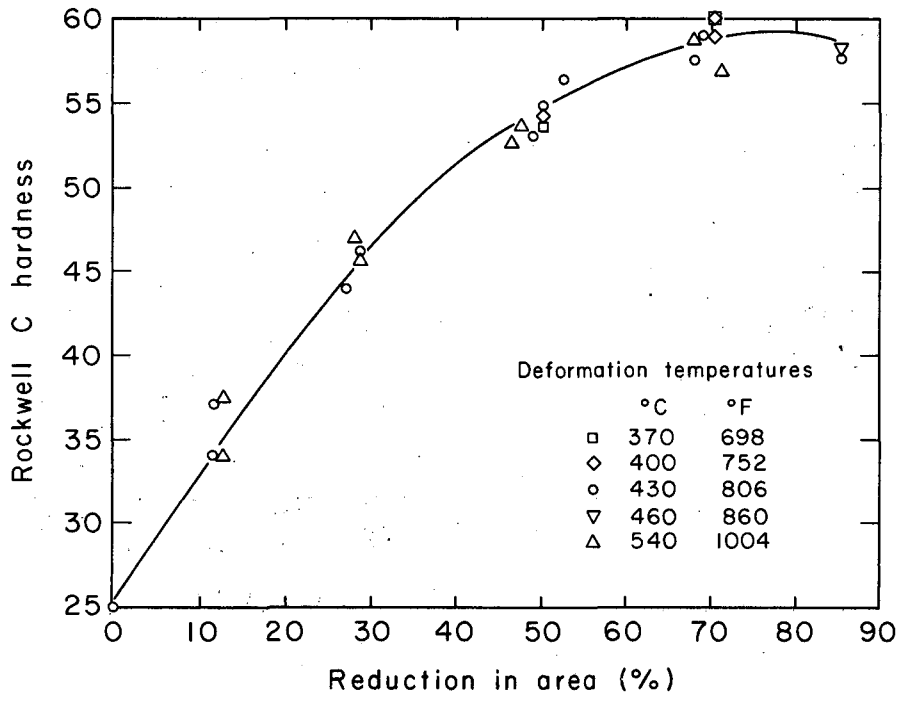

Fig. 3. The effect of deformation temperature and percent reduction in area on the hardness of as deformed austenite.

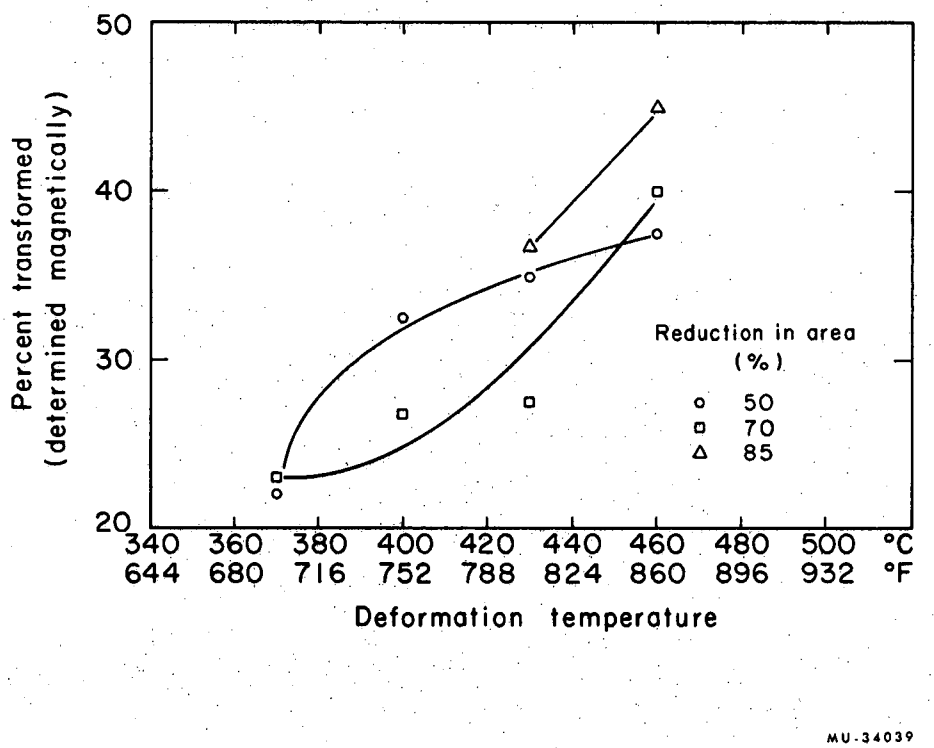

Fig. 4. The effect of deformation temperature and percent reduction in area on the extent of austenite to martensite transformation after cycle quenching to -196°C.

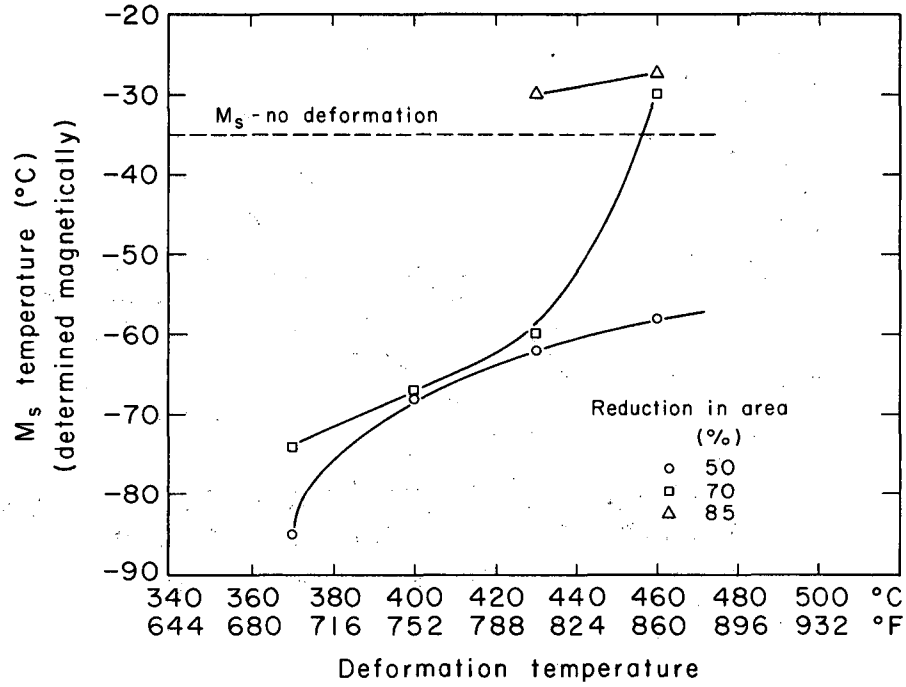

Fig. 5. The effect of deformation temperature and percent reduction in area on the Ms temperature.

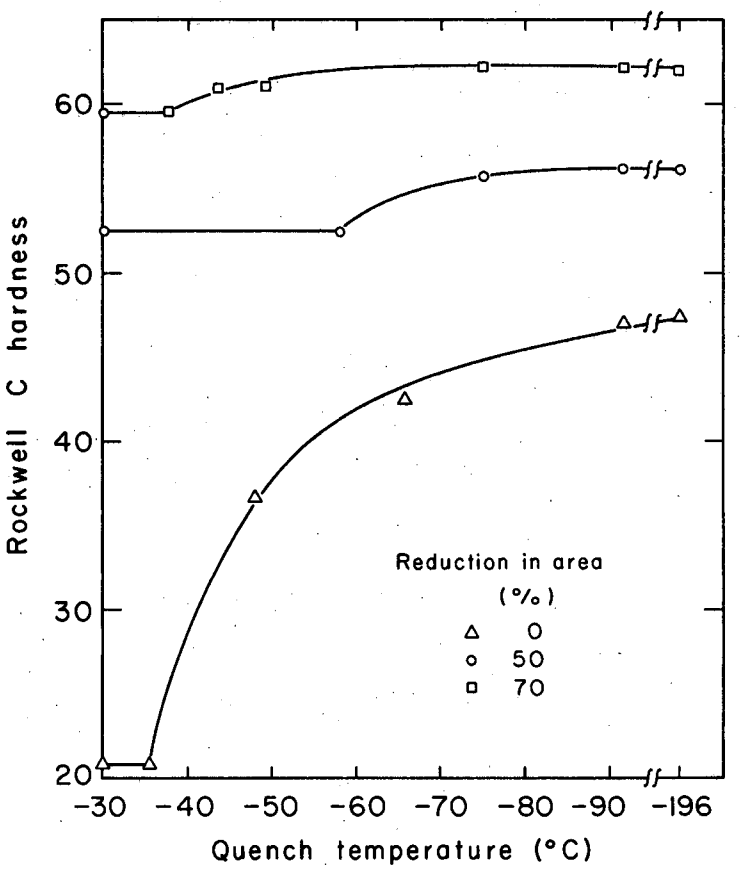

Fig. 6. The effect of the amount of deformation on the hardness after quenching to decreasing temperatures below the Ms. Deformation temperature 460°C (860°F); cycle tempering temperature 490°C (914°F); cycle tempering time 10 minutes.

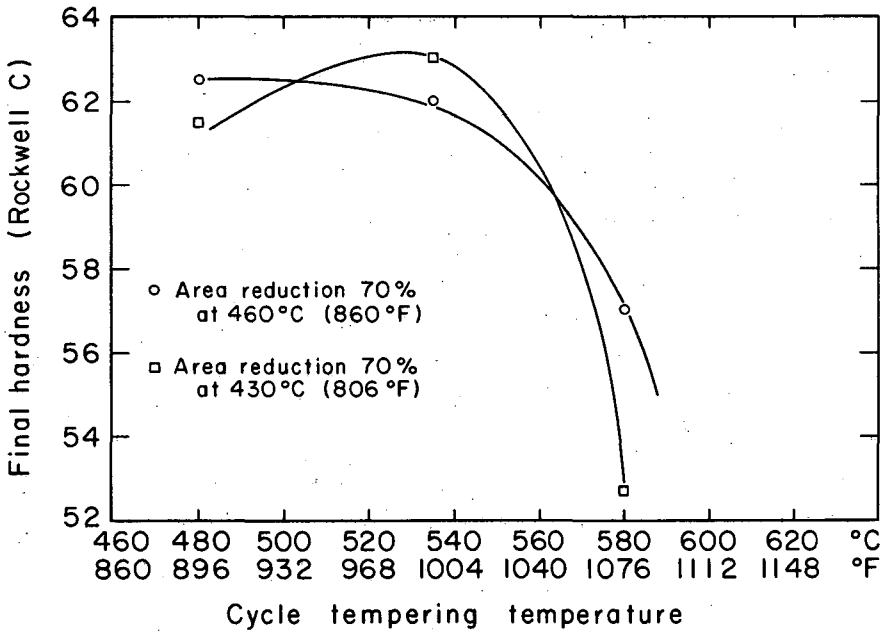

Fig. 7. The effect of cycle tempering temperature on the final hardness.

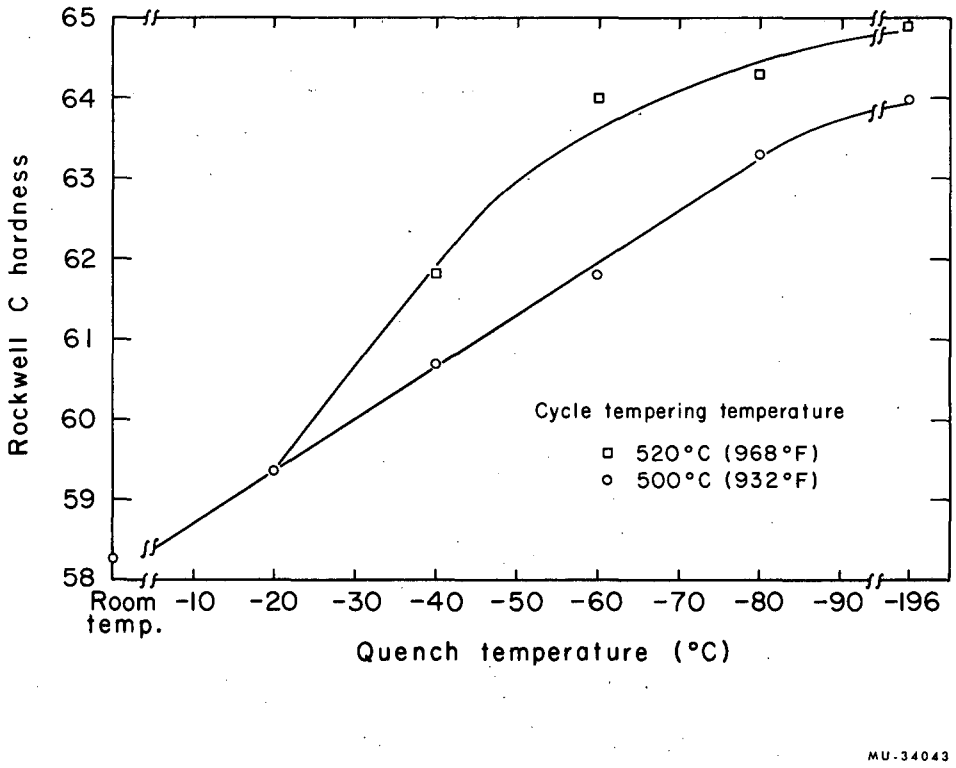

Fig. 8. The effect of cycle tempering temperature on the hardness after quenching to decreasing temperatures below the Ms. Area reduction 85 percent at 490°C (914°F).

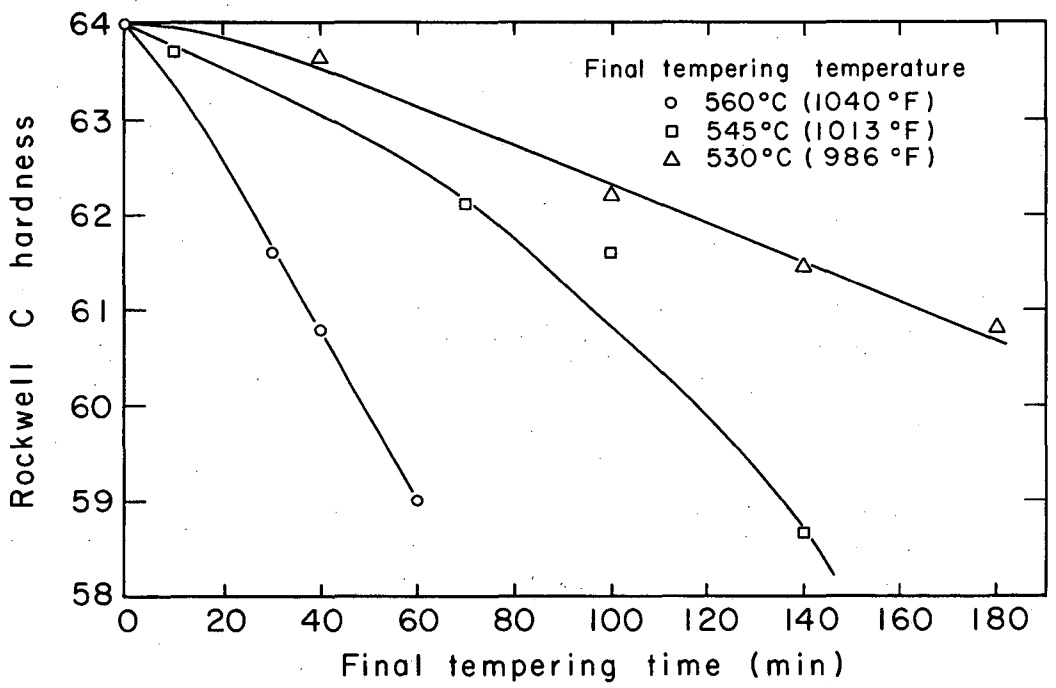

Fig. 9. The effect of time at various final tempering temperatures on the final hardness. Area reduction 85 percent at 490°C (914°F); cycle tempering temperature 500°C (932°F); cycle tempering time 10 minutes.

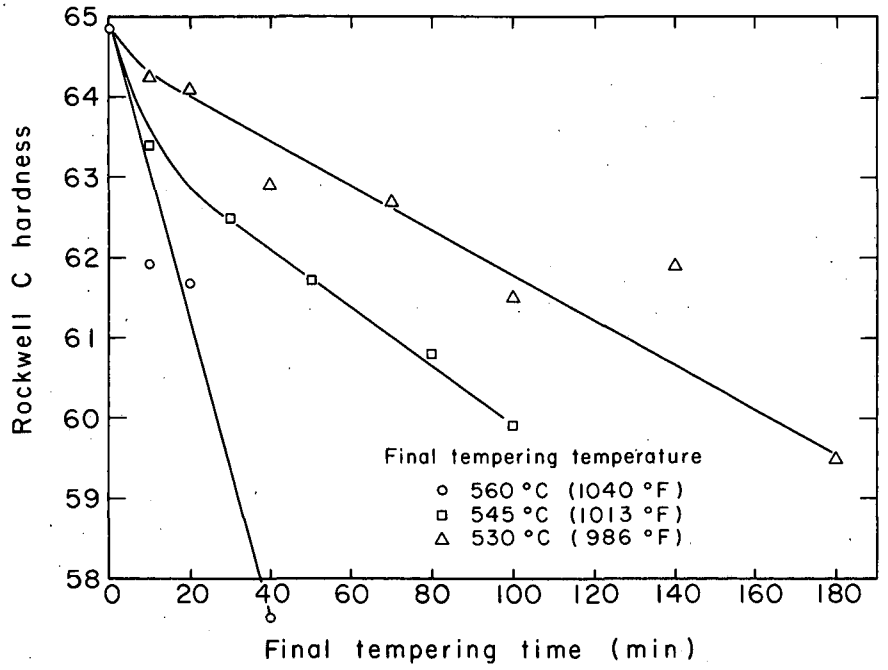

Fig. 10. The effect of time at various final tempering temperatures on the final hardness. Area reduction 85 percent at 490°C (914°F); cycle tempering temperature 520°C (968°F); cycle tempering time 10 minutes.

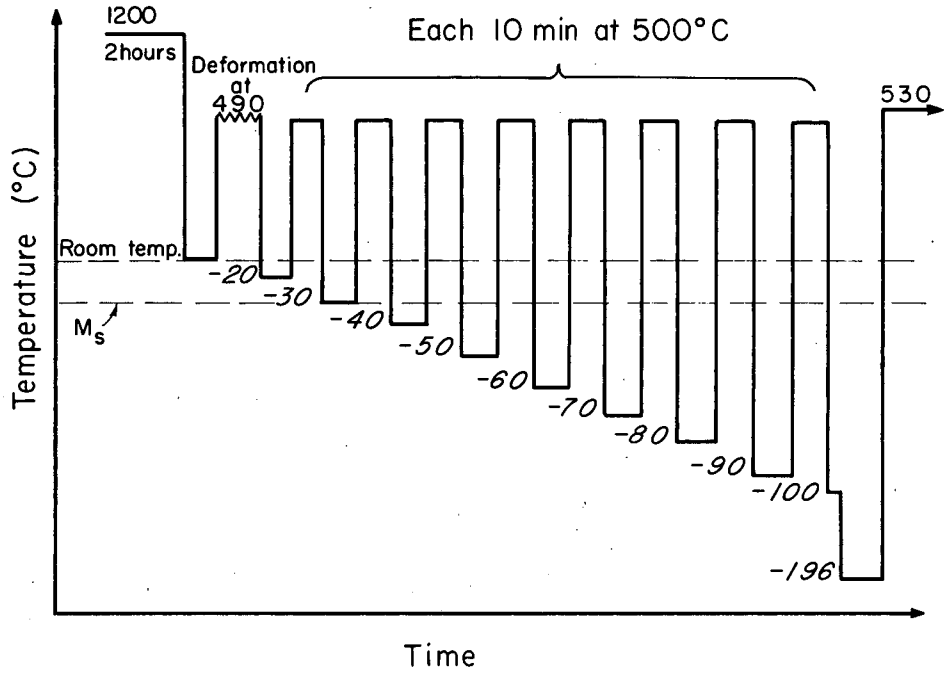

Fig. 11. Schematic representation of the final thermal-mechanical treatment.

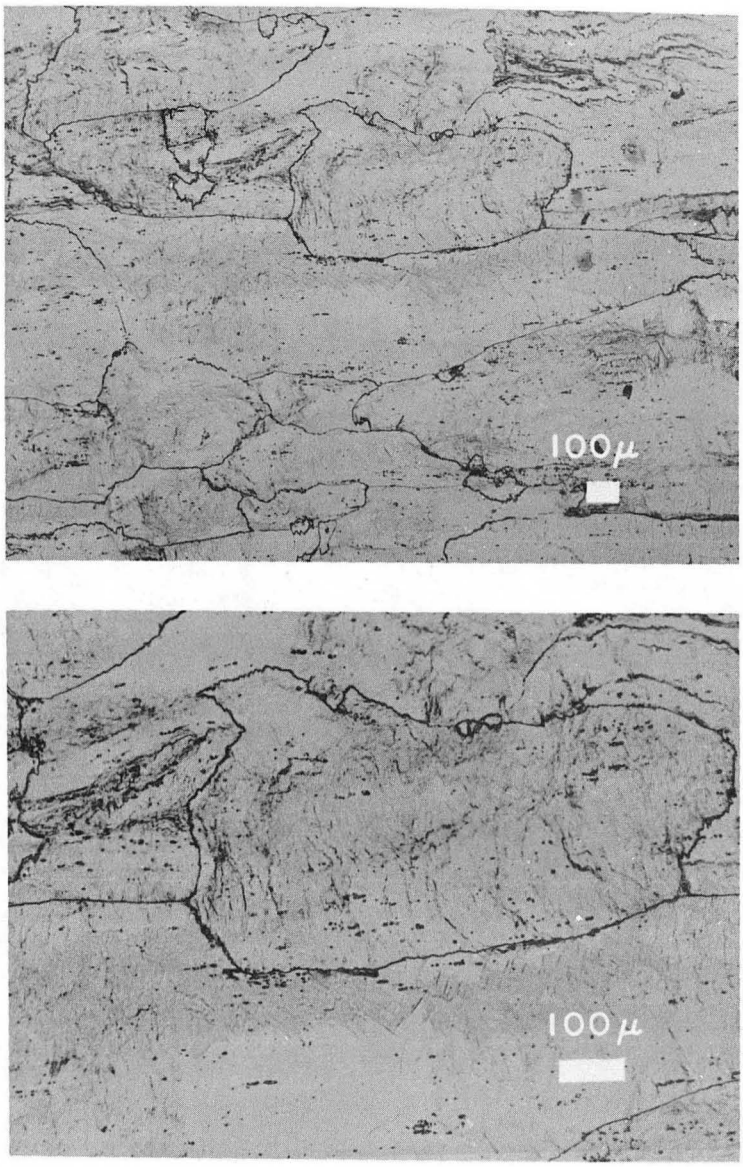

ZN-4309

Fig. 12. Deformed austenite. Same area in each photomicrograph, but at different magnifications. Etched in 5% nital for 60 minutes. Rolling direction from left to right.

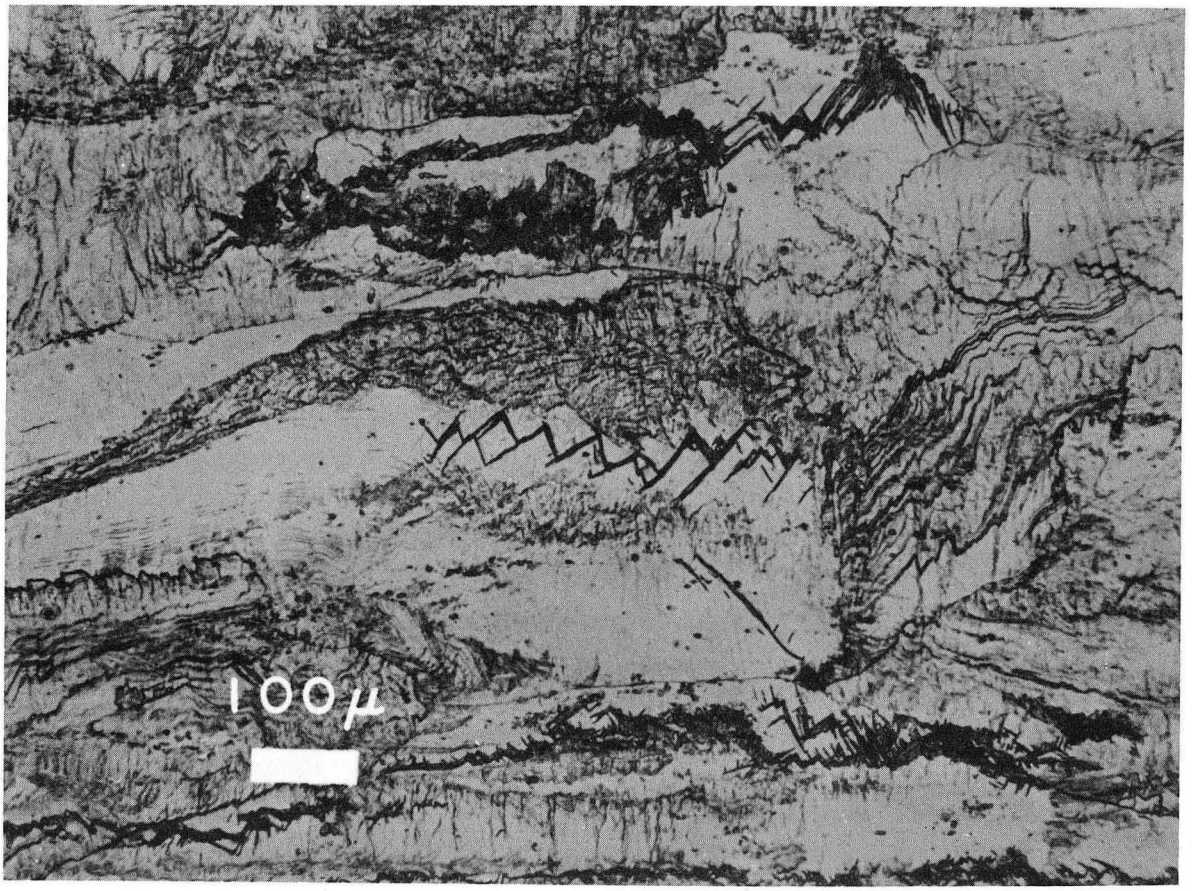

ZN-4310

Fig. 13. Deformed austenite treated as in Figure 11; cycle quenched to -20°C and tempered. Etched in 5% nital for 60 minutes. Rolling direction from left to right.

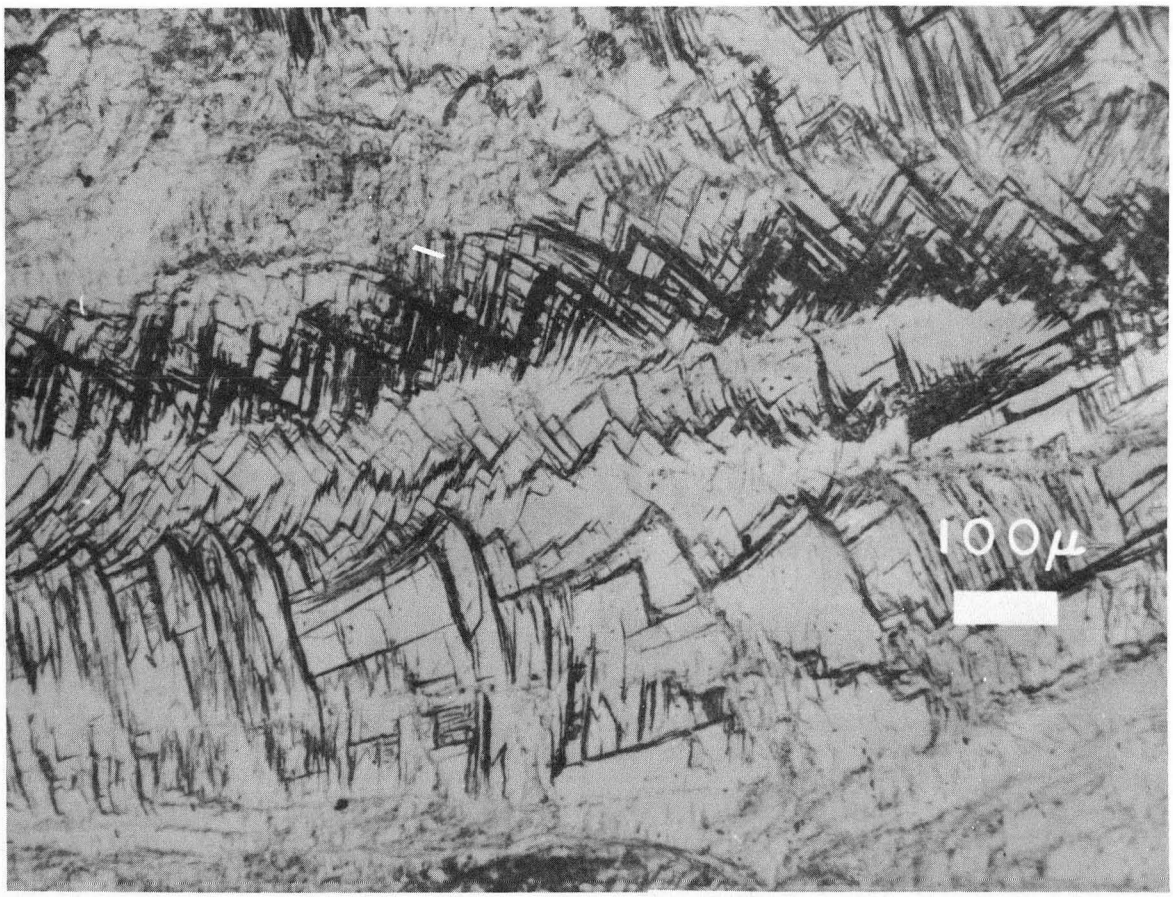

ZN-4311

Fig. 14. Deformed austenite treated as in Figure 11; cycle quenched to -40°C and tempered. Etched in 5% nital for 30 minutes. Rolling direction from left to right.

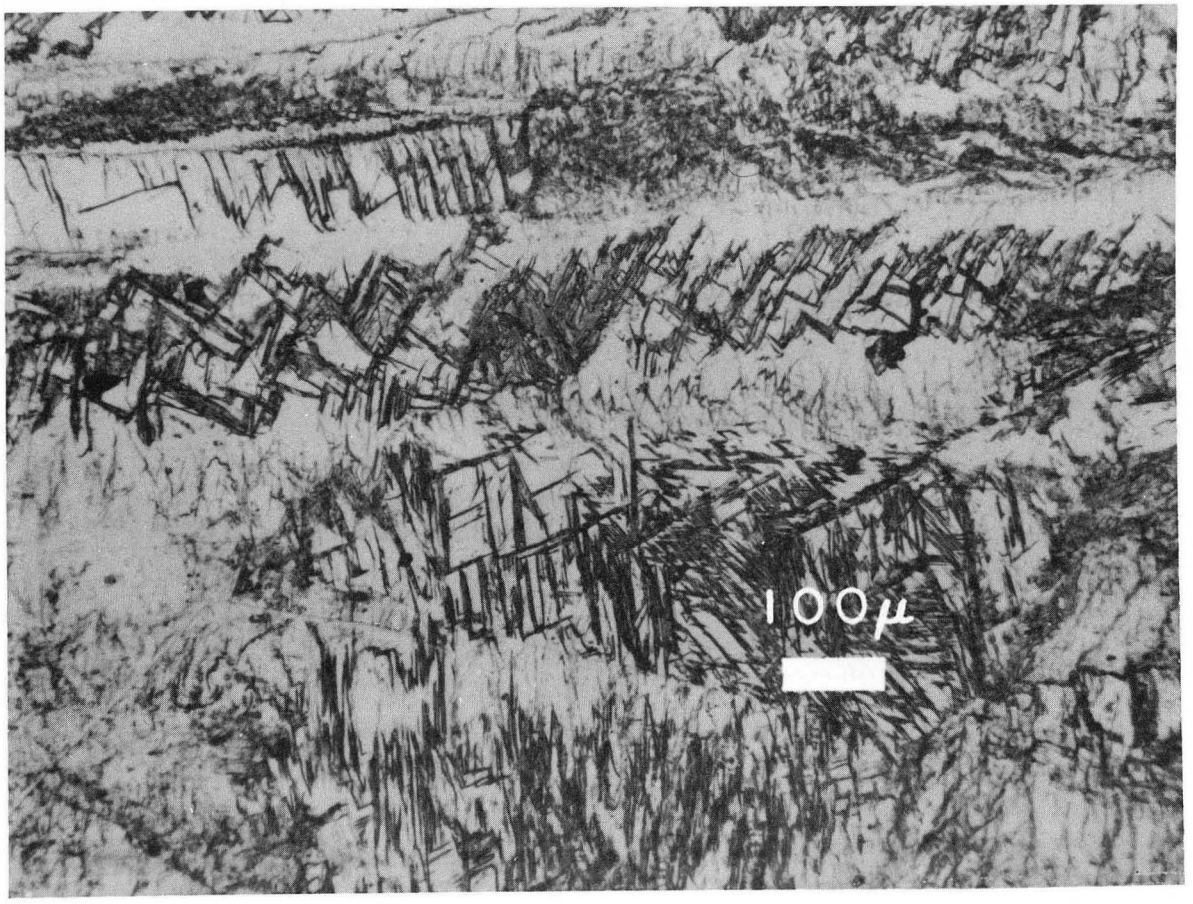

ZN-4312

Fig. 15. Deformed austenite treated as in Figure 11; cycle quenched to -60°C and tempered. Etched in 2% nital for 5 minutes. Rolling direction from left to right.

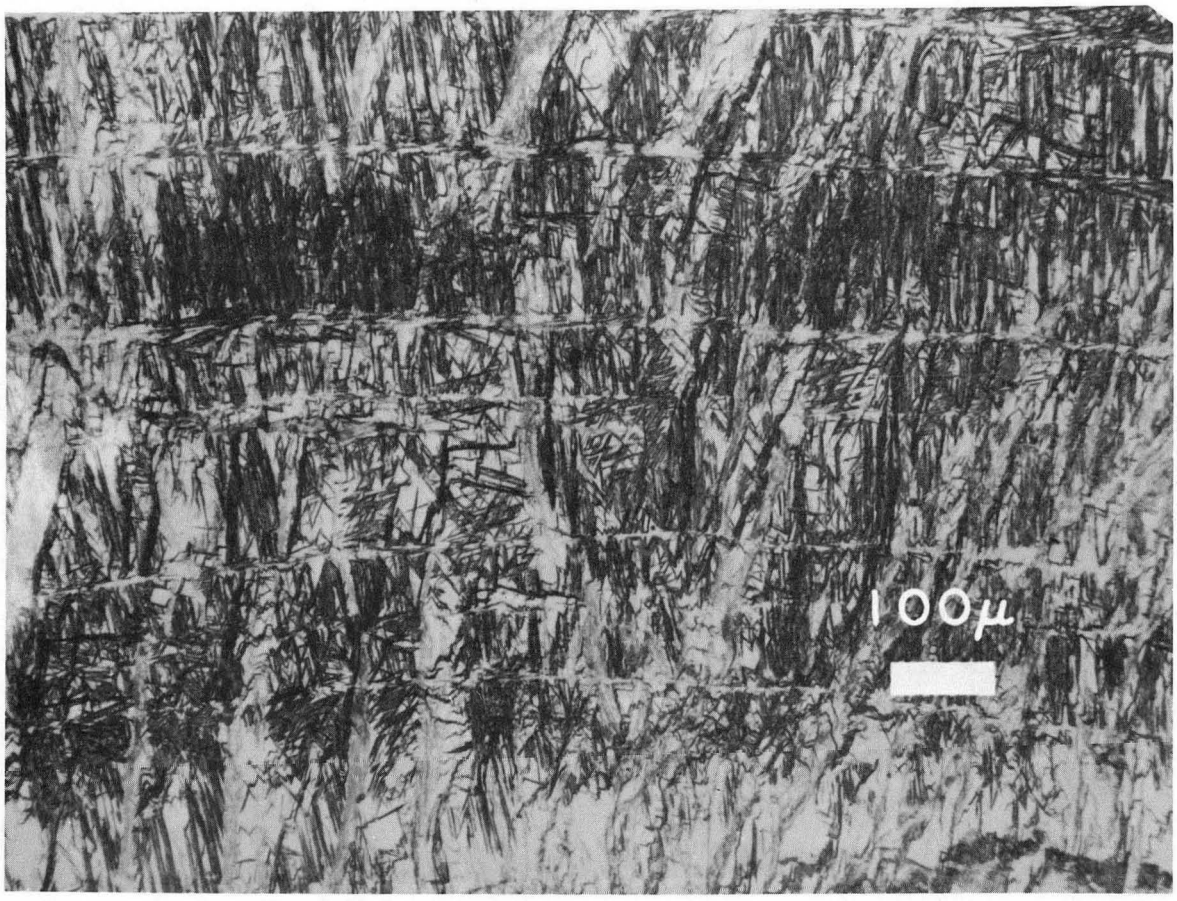

ZN-4313

Fig. 16. Deformed austenite treated as in Figure 11; cycle quenched to -80°C and tempered. Etched in 2% nital for 2 minutes. Rolling direction from left to right.

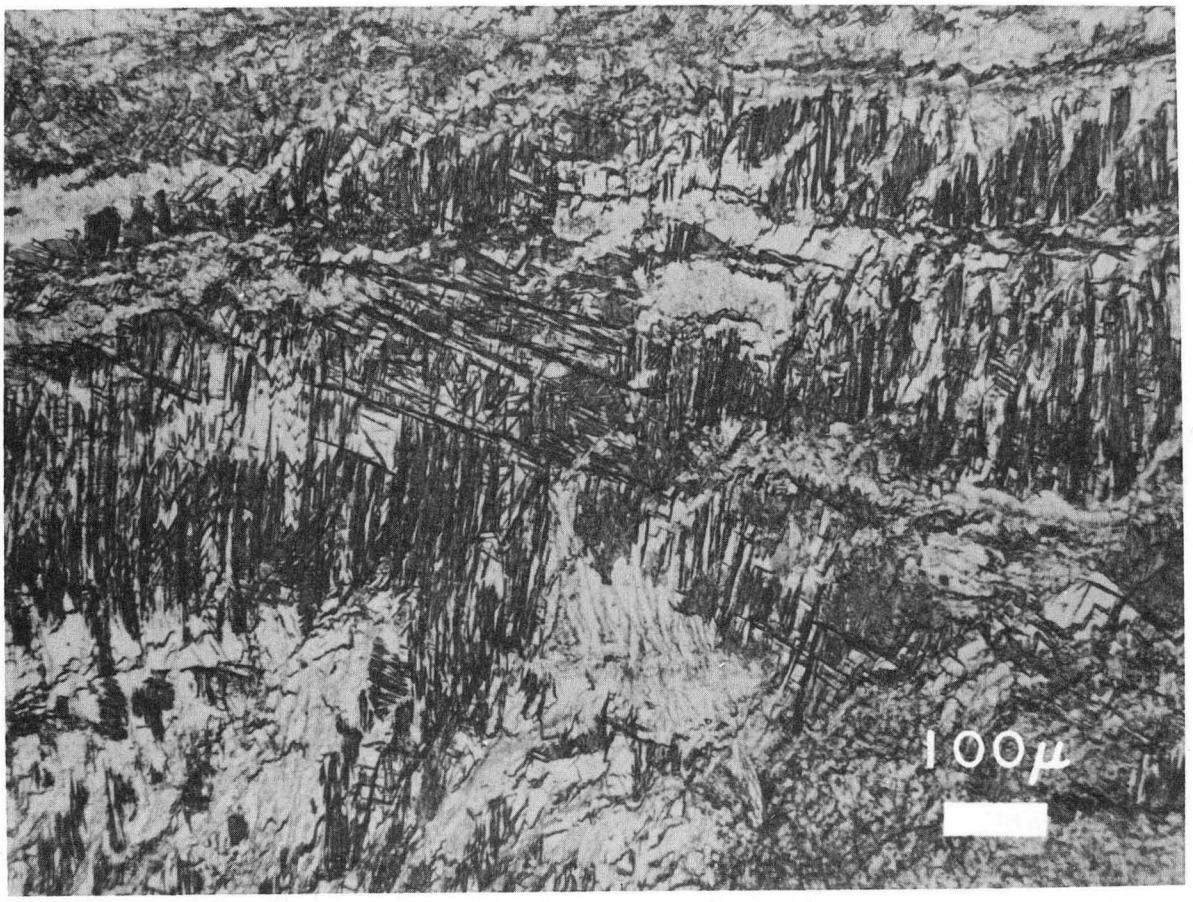

ZN-4314

Fig. 17. Deformed austenite treated as in Figure 11; cycle quenched to -196°C. Etched in 2% nital for 2 minutes. Rolling direction from left to right.

ZN-4315

Fig. 18. Undeformed austenite cycle quenched as in Figure 11 to -196°C. Etched in 2% nital for 10 minutes.

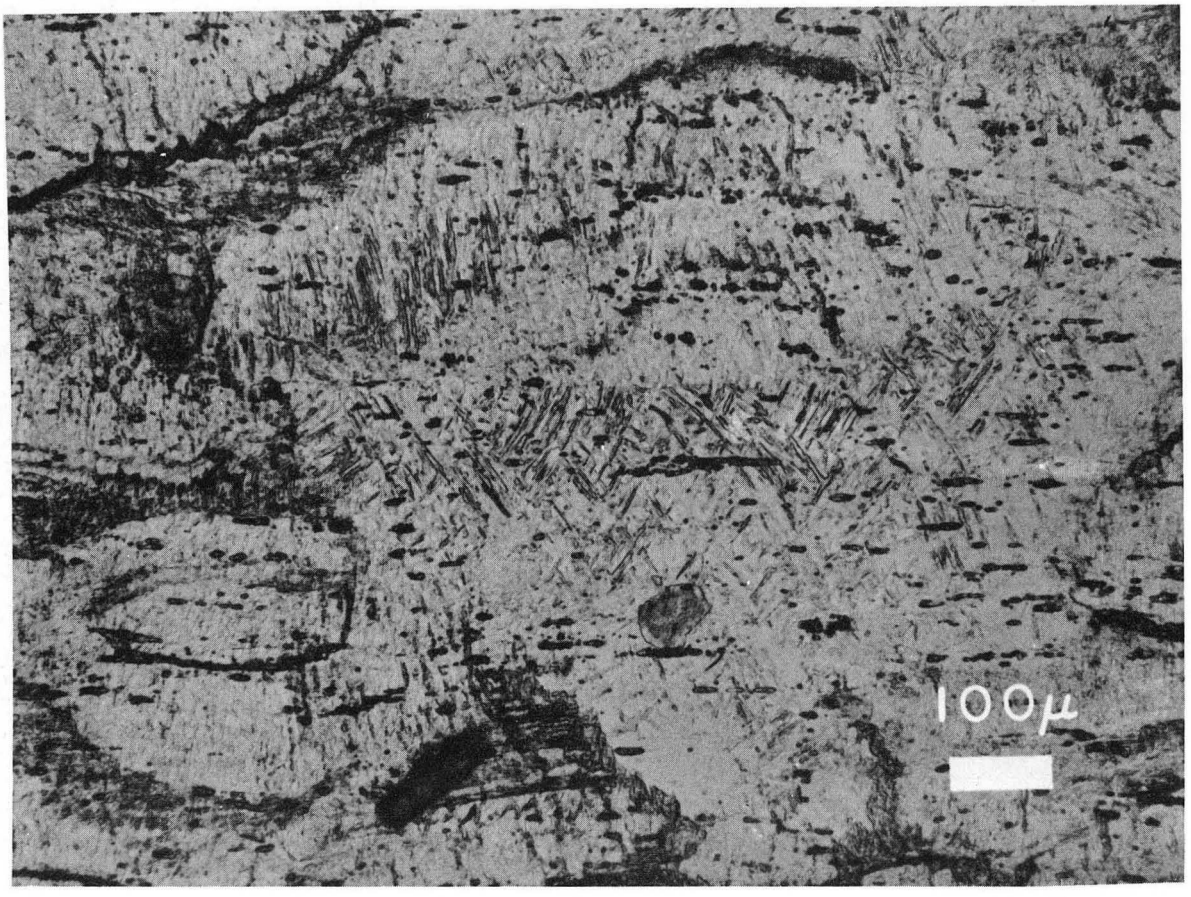

ZN-4316

Fig. 19. Deformed austenite (85 percent at 490°C) direct quenched to -196°C. Etched in 5% nital for 20 minutes. Rolling direction from left to right.

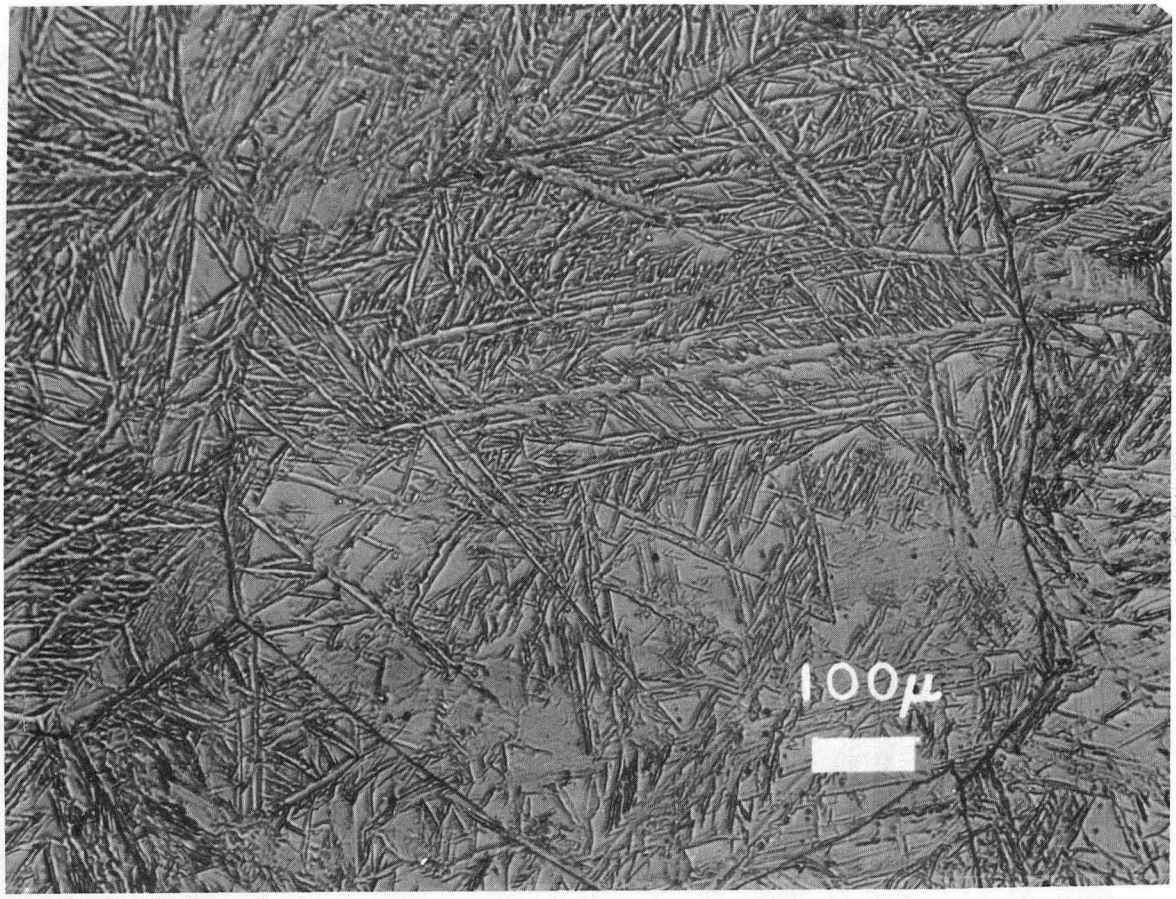

ZN-4317

Fig. 20. Undeformed austenite direct quenched to -196°C. Etched in 5% nital for 45 minutes.

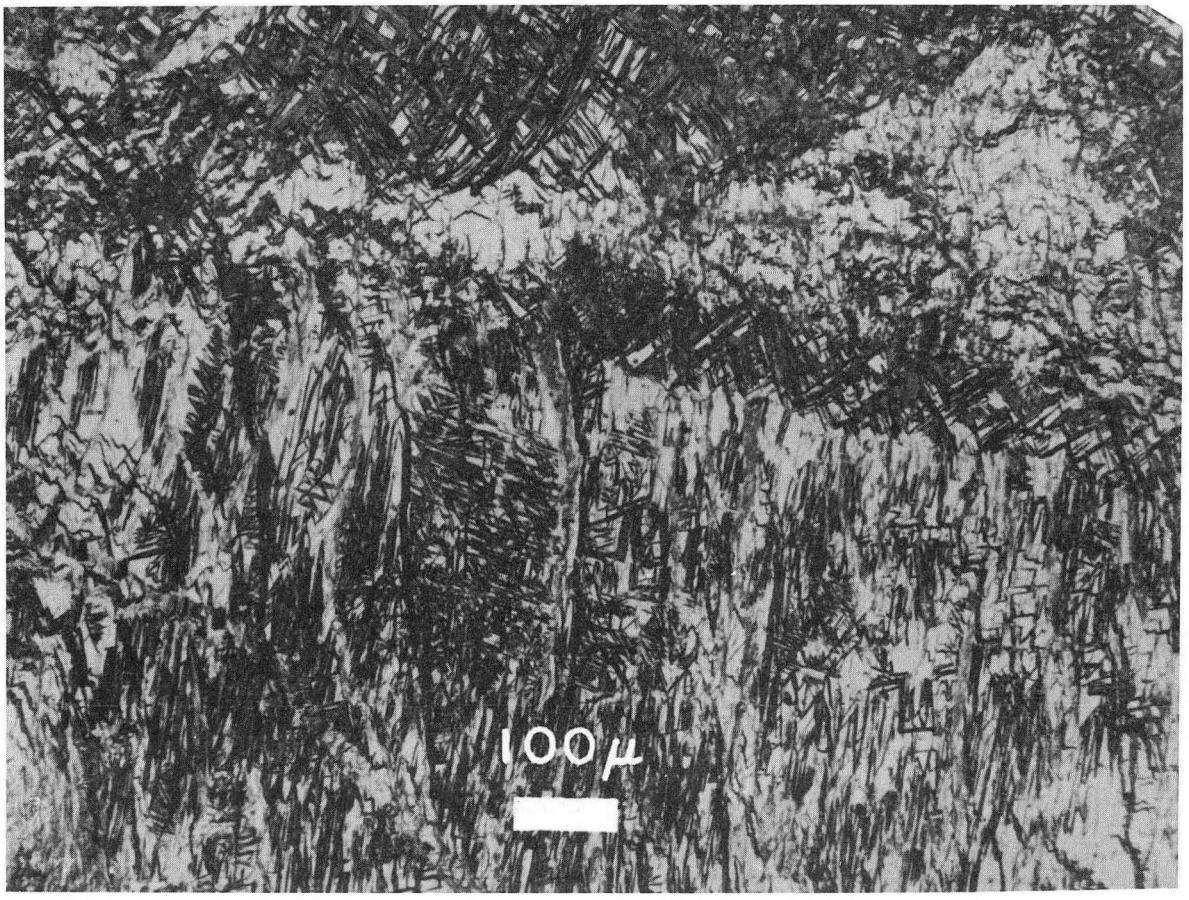

ZN-4318

Fig. 21. Deformed austenite treated as in Figure 11; and final tempered at 530°C (986°F) for one hour. Etched in 2% nital for 2 minutes. Rolling direction from left to right.

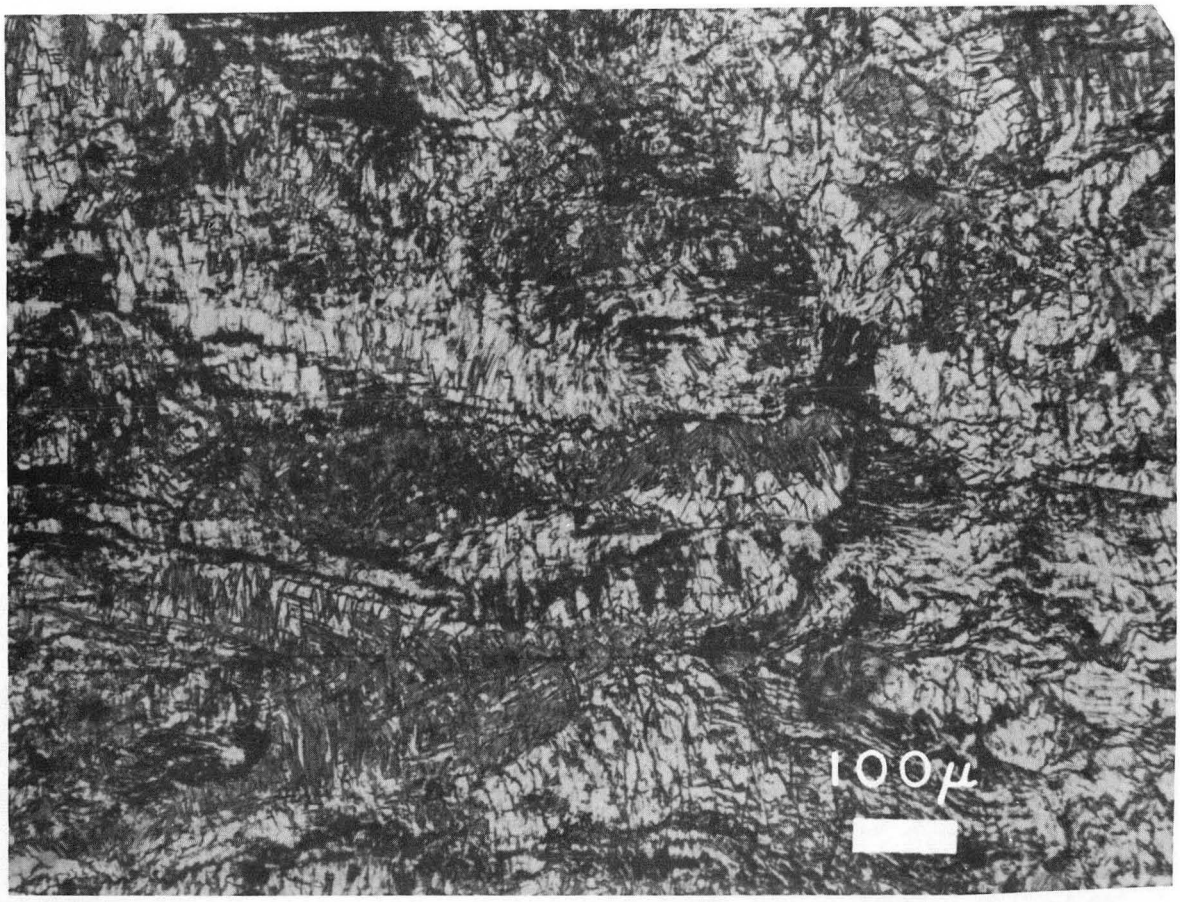

ZN-4319

Fig. 22. Deformed austenite treated as in Figure 11; and final tempered at 530°C (986°F) for three hours. Etched in 2% nital for 2 minutes. Rolling direction from left to right.

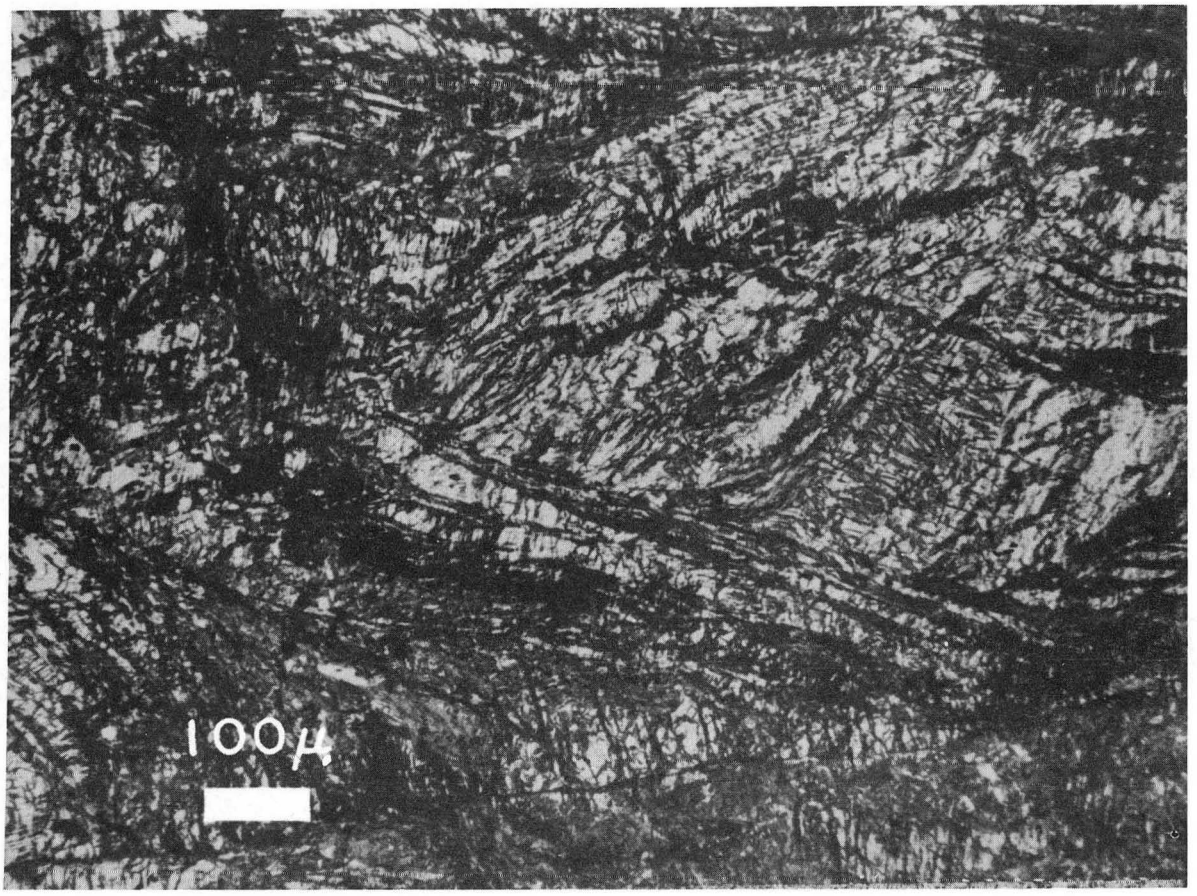

ZN-4320

Fig. 23. Deformed austenite treated as in Figure 11; and final tempered at 530°C (986°F) for five hours. Etched in 2% nital for 2 minutes. Rolling direction from left to right.

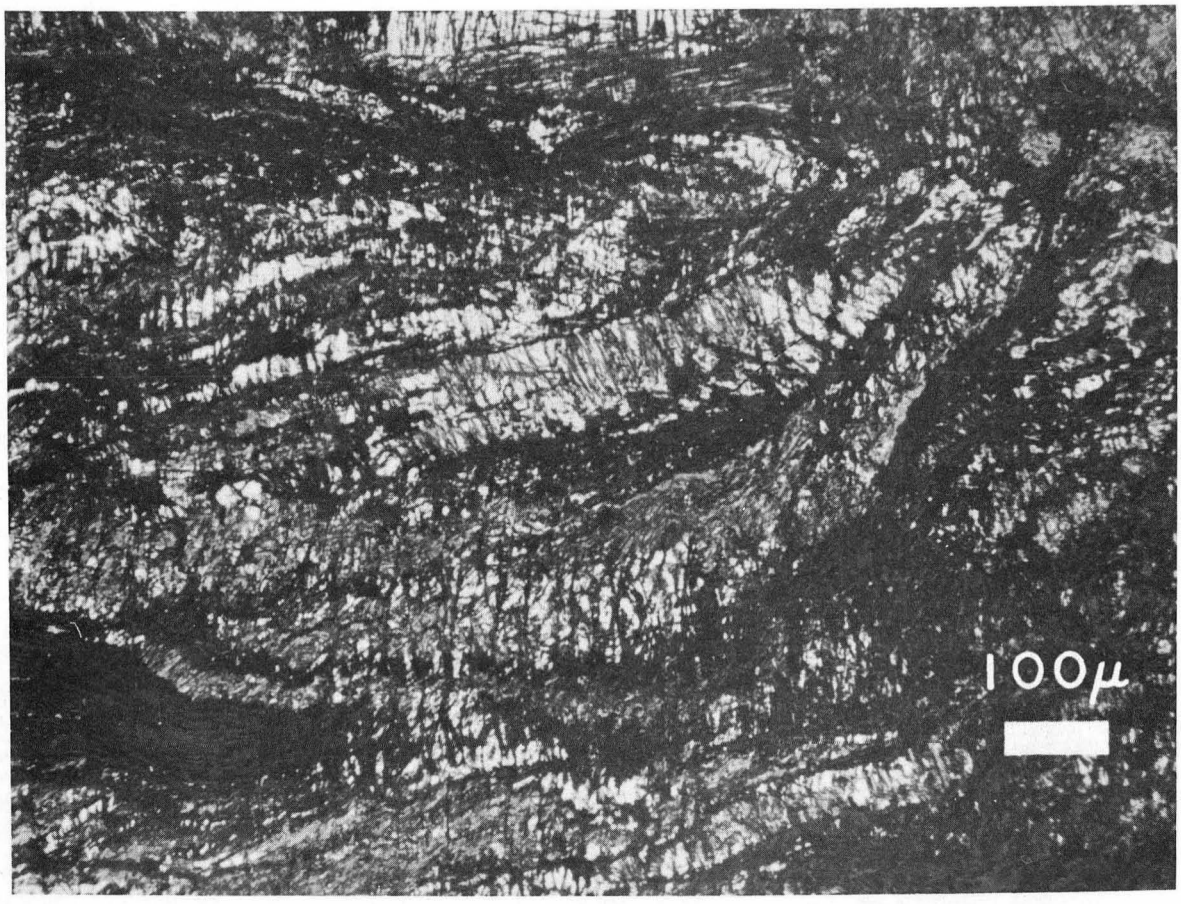

ZN-4321

Fig. 24. Deformed austenite treated as in Figure 11; and final tempered at 530°C (986°F) for seven hours. Etched in 2% nital for 2 minutes. Rolling direction from left to right.

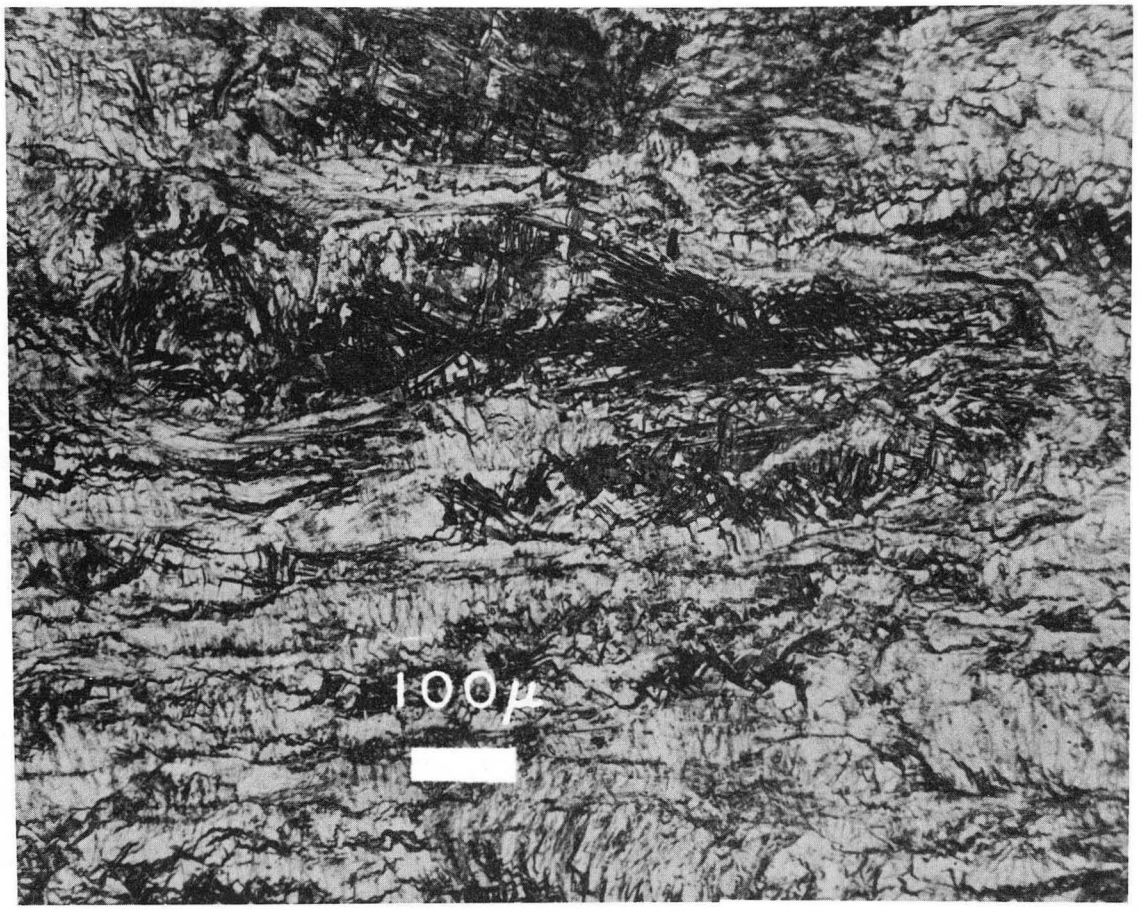

ZN-4322

Fig. 25. Austenite deformed 70 percent at 490°C (914°F), and cycle quenched to -196°C. Etched in 2% nital for 2 minutes. Rolling direction from left to right.

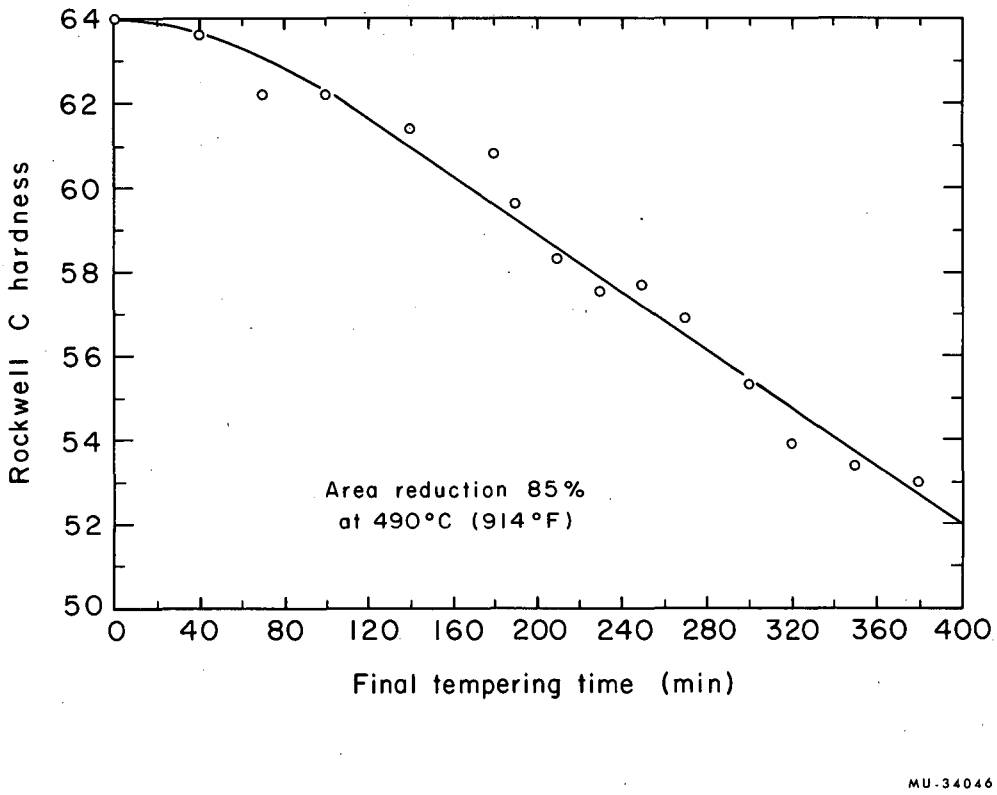

Fig. 26. The effect of final tempering temperature on the hardness of austenite treated as in Figure 11; and final tempered at 530°C (986°F).

Table I.

Deformation Temperature	Reduction in Area	Cycle Tempering Temperature	Final Tempering Treatment	Tensile Strength psi x 10^{-3}	Ductility %
430	85	550	None	220	2
460	85	510	"	260	< 1
460	85	550	"	220	1.5
490	85	510	"	340	2
490	85	550	"	280	4

ACKNOWLEDGEMENTS

The author wishes to express his appreciation to Professor E. R. Parker and Dr. V. F. Zackay, Department of Mineral Technology, University of California, for their helpful discussions and counsel throughout the course of this investigation. The author also wishes to express his appreciation to Mr. George Blank for his help in initiating this investigation, and to Mrs. Rosa Nissen for her help in preparing samples used in this investigation.

The author also expresses his thanks to the Inorganic Materials Research Division of the Lawrence Radiation Laboratory, University of California, for its financial assistance, without which this research could not have been accomplished.

This work was performed under the auspices of the United States Atomic Energy Commission.

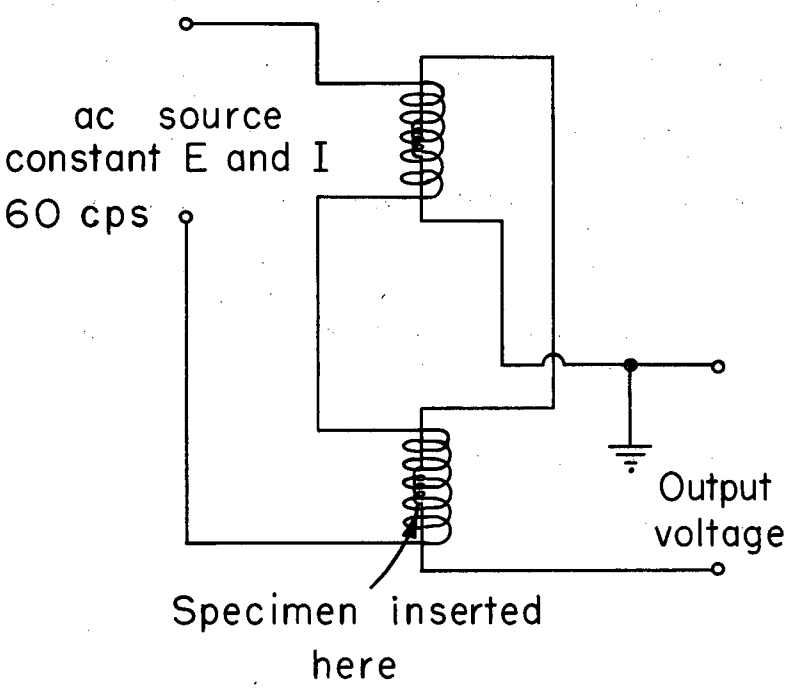

Fig. Appendix A

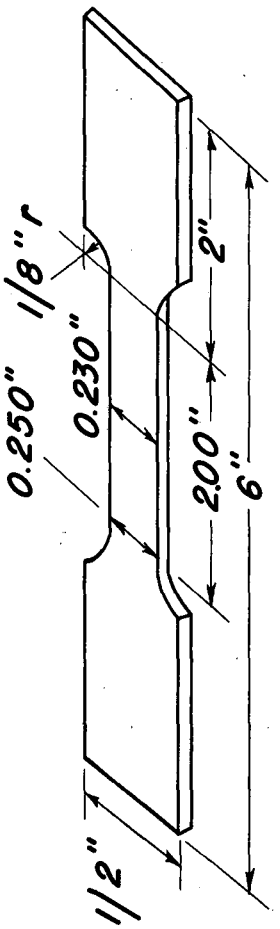

Thickness 0.040"

MU-34075

Fig. Appendix B

BIBLIOGRAPHY

1. E. Orowan, "Dislocations and Mechanical Properties," in Dislocations in Metals, ed. M. Cohen, AIME, New York, 1954, p. 69.

2. A. M. Turkalo and J. R. Low, Jr., "The Effect of Carbide Dispersion on the Strength of Tempered Martensite," Trans. AIME, 212, 750 (1958).

3. A. J. McEvily and R. H. Bush, "An Investigation of the Notch-Impact of an Ausformed Steel," Trans. ASM, 55, 654 (1962).

4. A. J. McEvily, R. H. Bush, F. W. Schaller and D. J. Schmatz, "On the Formation of Alloy Carbides During Ausforming," Trans. ASM, 56, 735 (1963).

5. D. J. Schmatz, F. W. Schaller and V. F. Zackay, "Structural Aspects and Properties of Martensite of High Strength," The Relation Between Structure and Mechanical Properties of Metals, National Physical Laboratory, Symposium No. 15, London, Her Majesty's Stationery Office 1963.

6. W. M. Justusson and D. J. Schmatz, "Some Observations on the Strength of Martensite Formed form Cold-Worked Austenite," Trans. ASM, 55, 640 (1962).

7. D. V. Wilson, "Effect of Plastic Deformation on Carbide Precipitation in Steel," Acta Met., 5, 293 (1957).

8. A. H. Cottrell, Report on Strength of Solids, Phys. Soc, 1948, p. 30.